www.ptcer.pl/mccm

MATERIAŁY CERAMICZNE /CERAMIC MATERIALS/, 68, 2, (2016), 176-182

Modeling of thermal residual stresses in the SiC-TiB_2 composite system considering real microstructure and thermo-mechanical properties anisotropy

Grzegorz Grabowski*, Zbigniew Pędzich

AGH University of Science and Technology, Faculty of Materials Science and Ceramics, Department of Ceramics and Refractory Materials, al. A. Mickiewicza 30, 30-059 Kraków, Poland
*e-mail: grzegorz.grabowski@agh.edu.pl

Abstract

The results are presented concerning simulations of the distribution of thermal residual stresses in a ceramic matrix particulate-reinforced composite in the SiC-TiB_2 system. The stresses arise during cooling of the material after sintering due to differences in thermal expansion and elastic properties of the component phases, and belong to the most important factors for increasing fracture toughness of ceramic composites. A computational model was built on the basis of the real microstructure of the SiC-TiB_2 composite. The material properties of component phases used in calculations included their temperature dependences. A temperature difference caused shrinkage and residual stress was adopted by means of the analysis of the sintering curves. The simulations were performed by using the finite element method. The results of simulations were compared with the calculated values of residual stresses, basing on analytical models and experimental data. The comparison shows good agreement. This allows an elaborated model to be used to solve more complex problems concerning fracture analysis of ceramic matrix composites.

Keywords: SiC-TiB_2, Ceramic matrix composites, Fracture toughness, Thermal residual stress, Finite element method

MODELOWANIE CIEPLNYCH NAPRĘŻEŃ RESZTKOWYCH W KOMPOZYTACH Z UKŁADU SiC-TiB_2 Z UWZGLĘDNIENIEM RZECZYWISTEJ MIKROSTRUKTURY I ANIZOTROPII WŁAŚCIWOŚCI TERMO-MECHANICZNYCH

Zaprezentowano wyniki dotyczące symulacji rozkładu cieplnych naprężeń resztkowych w kompozycie dyspersyjnych z osnową ceramiczną z układu SiC-TiB_2. Naprężenia powstały podczas studzenia materiału po spieczeniu z powodu różnic w rozszerzalności cieplnej i właściwościach sprężystych składowych, a należą one do najważniejszych czynników odpowiedzialnych za zwiększenie odporności na pękanie kompozytów ceramicznych. Model obliczeniowy został zbudowany na bazie rzeczywistej mikrostruktury kompozytu SiC-TiB_2. Właściwości materiałowe składowych faz użyte w obliczeniach uwzględniały ich zależność od temperatury. Różnica temperatury powodująca skurcz i naprężenia resztkowe została uzyskana za pomocą analizy krzywych spiekania. Symulacje przeprowadzono z wykorzystaniem metody elementów skończonych. Otrzymane wyniki porównano z wynikami obliczeń naprężeń resztkowych opartych na modelach analitycznych i danych eksperymentalnych, uzyskując dobrą zgodność, co pozwoliło na opracowanie modelu użytecznego do rozwiązywania bardziej skomplikowanych problemów dotyczących analizy pękania kompozytów z osnową ceramiczną.

Słowa kluczowe: SiC-TiB_2, kompozyty z osnową ceramiczną, odporność na pękanie, cieplne naprężenia resztkowe, metoda elementów skończonych

1. Introduction

Silicon carbide belongs to the group of materials with a dominant covalent bond. It causes that SiC has very high hardness, high temperature creep resistance and very good chemical stability. The wider application of SiC as a structural material is limited due to its relatively low fracture toughness (K_{IC} = 2-5 MPa·$m^{0.5}$ [1-3]). The toughening effect in SiC can be reached by the modification of its composition. Incorporation of inclusions into SiC matrix can put into motion some additional mechanisms that increase fracture energy.

Particulate composites in the SiC-TiB_2 system are the materials showing improved fracture toughness. Final values of K_{IC} depend on the volume fraction of TiB_2 and can reach even 6-8 MPa·$m^{0.5}$ [4-6]. The fracture energy increase in the composites compared to single phase SiC is connected with some additional processes such as: the crack deflection, crack bridging, creation of microcracks and influence of residual thermal stress on a crack propagating through the material [4, 7-13]. The level of influence of each individual mechanism is not recognized quantitatively. Depending on inclusion and matrix size and shape, some mechanisms could affect positively the fracture toughness and others affect them negatively.

One of the main factors, decisive for the effectiveness of the toughness increase mechanisms is constituted by the presence of residual thermal stress in the material. Despite

the direct interaction of a crack with the stresses cumulated near the crack tip [8], they influence crack deflection [14], crack bridging or microcracking [8, 9, 12].

The evaluation of the residual thermal stresses in the SiC-TiB_2 composite can be done using the experimental data [15, 16] or by means of analytical solutions [8, 17]. The valuable data, coming from direct measurements, have a relatively large level of uncertainty caused by difficulties with the proper preparation of samples. Stress values measured experimentally have a relatively large dispersion. The analytical solutions do not consider the grain shape and properties anisotropy, coming from the crystallographic structure of composite compounds.

In the presented work the finite elements method was applied to determine the thermal residual stress distribution in the SiC-TiB_2 composite. These results were used for elaborating the model basing on the real microstructure. The influence of grain shape and their anisotropy on the stress values was analysed.

2. Experimental

2.1. Material

The dense polycrystalline composite material in the SiC-TiB_2 system was prepared by hot-pressing. Raw materials comprised a silicon carbide powder (H. C. Starck, UF-15) and boron titanium one (GE Advanced Ceramics, HCT-S). The compounds were used in a proportion of 20 vol.% TiB_2 and 80 vol.% SiC. Additionaly, SiC sintering activators were used: 0.5 wt.% of amorphous boron (Fluka Cat. No. 15580) and 3 wt.% carbon (phenol-formaldehyde resin by Novolak Organika-Sarzyna) [18, 19]. Sintering was conducted at 2150°C under a pressure of 25 MPa in the argon atmosphere. Apparent density of sintered bodies reached ~99% of the theoretical one.

The images of composite microstructures were taken from polished surfaces by a camera using the optical microscope. Such images were used for the preparation of a geometric model.

2.2. Microstructure model

The analysis of the residual thermal stress was performed for a selected area of 2250 μm^2 which contained 54 TiB_2 grains. Their volume fraction was 19.6%. The matrix microstructure was generated synthetically in two variants. The first one assumed the bi-modal grain shape distribution (Fig. 2a). The matrix consisted of elongated grains with an average aspect ratio of ~5, and their volume content was 50%. The rest of the matrix grains were isometric with an average aspect ratio of ~1. In the second variant the elongated grains of SiC were divided and the matrix was composed of isometric grains with an average aspect ratio of ~1 only (Fig. 2 b).

The values of the thermal residual stress calculated using the numerical mode were compared with the values calculated on the Taya equations base [8]. The model basing only on a synthetic microstructure was also prepared. It consisted of a uniform SiC matrix with circular TiB_2 grains in the amount of 20 vol.% (Fig. 2c).

2.3. Mechanical characterisation

Both α-SiC and TiB_2 shows the hexagonal crystal structure. Single crystallites (grains) of the model composite are anisotropic. Giving consideration for this phenomenon demanded an experimental determination of elastic constants C_{ij} [20, 21] (Table 1). These constants were only slightly dependent on temperature, so typical values were assumed in the temperature range of 25-1200°C. In this temperature range the decrease in elastic moduli E, G is (6-7)% for both SiC and TiB_2 [1, 22, 23]). The modelling with the assumption of isotropic properties of constituent phases used Young's modulus (E), shear modulus (G) and Poisson's ratio (v) calculated from the same elastic constants as in case of the anisotropic model. They were calculated as the Voigt-Reuss mean value from the equations proposed by Hill [24] for the isotropic polycrystals (Table 1).

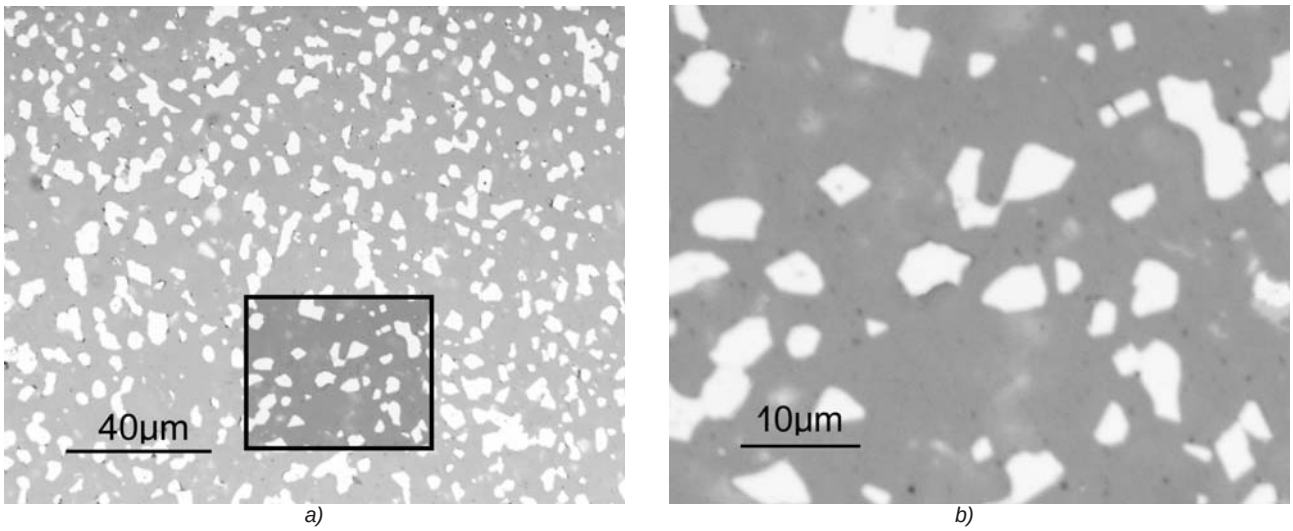

a) b)

Fig. 1. Microstructures of SiC-TiB_2 composite: a) image of microstructure chosen for analyse, b) part of image (a) used for geometrical model preparation.

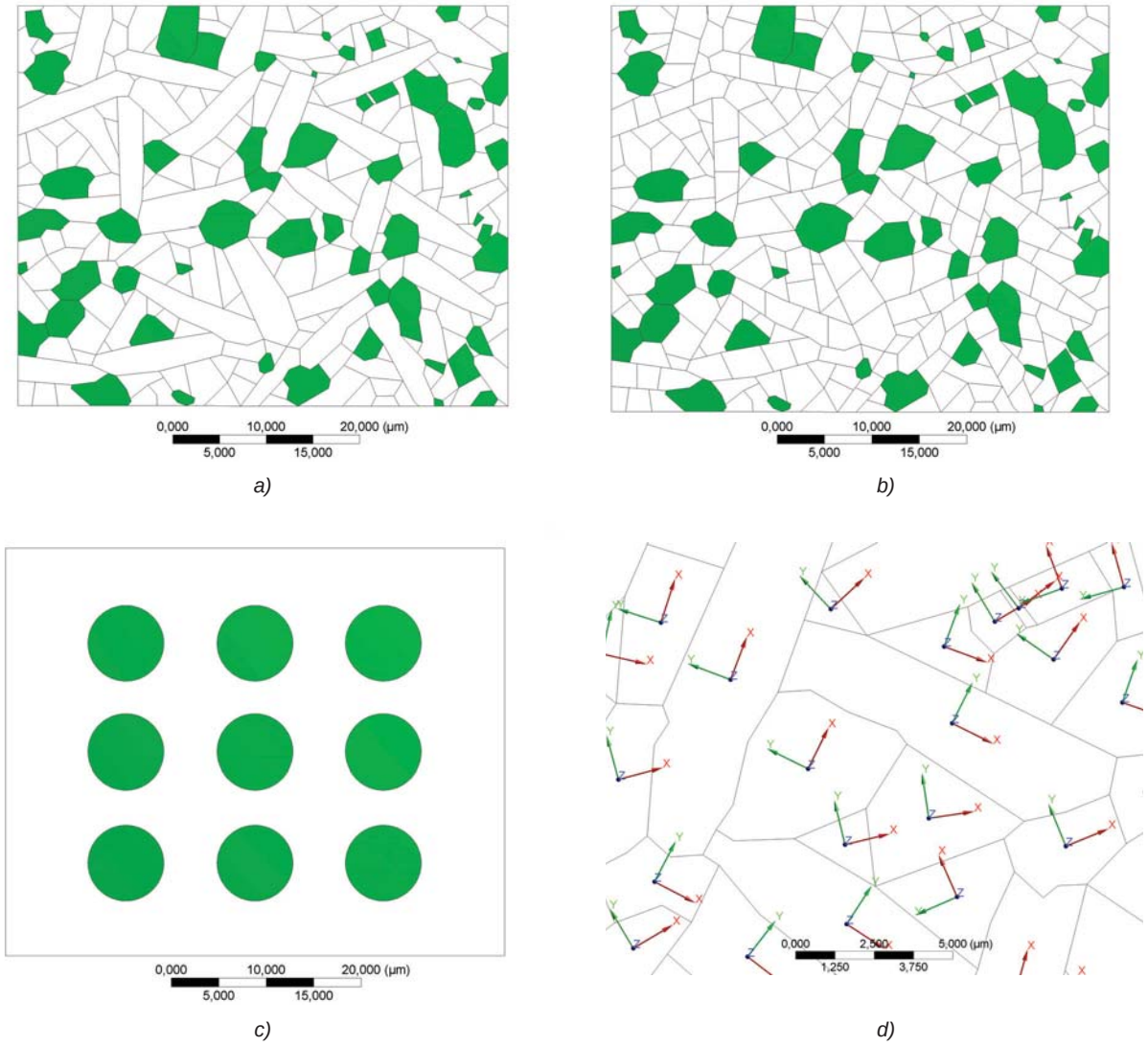

Fig. 2. Geometrical models used for thermal residual stress distribution analysis:
a) elongated matrix grains, b) isometric matrix grains, c) circular reinforcement particles, d) local coordinate system (LCS).

Table 1. Material characteristics used for modelling.

Mechanical properties										
	C_{11} [GPa]	C_{12} [GPa]	C_{13} [GPa]	C_{33} [GPa]	C_{44} [GPa]	$E_{VRH}^{(a)}$ [GPa]	$G_{VRH}^{(a)}$ [GPa]	$\nu_{VRH}^{(a)}$	d [kg/m^3]	
α-SiC [1, 20]	479	98	56	522	148	419	179	0.17	3.214	
TiB_2 [21, 23]	660	48	93	432	260	579	262	0.10	4.500	
Thermal expansions										
		25°C	100°C	200°C	400°C	600°C	800°C	1000°C	1200°C	
α-SiC [25,26]	CTE a-axis [10^{-6} 1/°C]	3.5	3.7	3.9	4.3	4.6	4.9	5.2	5.4	
	CTE c-axis [10^{-6} 1/°C]	3.3	3.5	3.7	4.0	4.3	4.5	4.8	4.9	
TiB_2 [27]	CTE a-axis [10^{-6} 1/°C]	4.7	5.0	5.5	6.3	7.1	7.7	8.3	8.8	
	CTE c-axis [10^{-6} 1/°C]	7.5	7.8	8.3	9.1	9.8	10.4	10.9	11.3	

[(a)] values calculated in this work

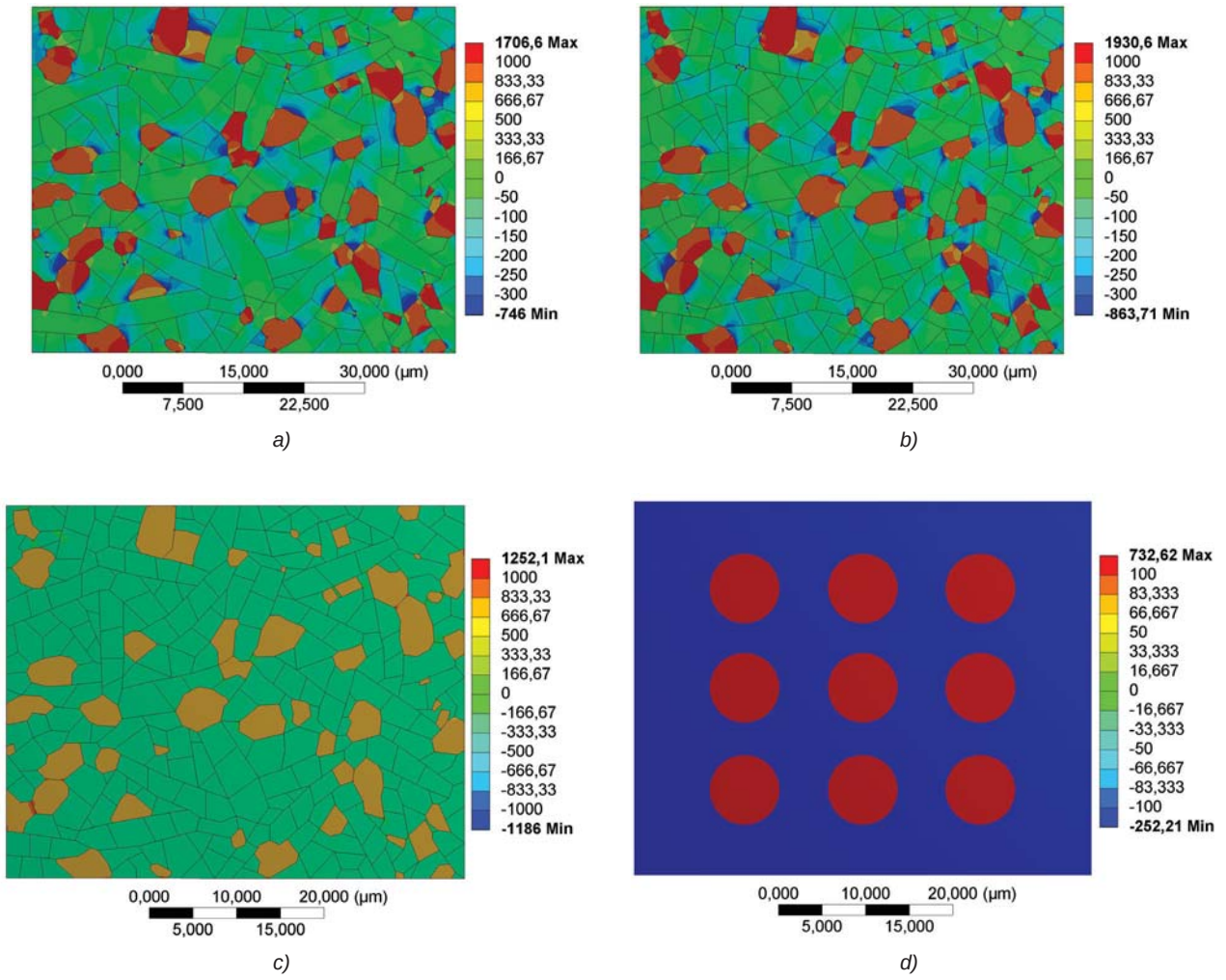

Fig. 3. Results of performed simulations as average hydrostatic stress $\sigma_h = (\sigma_x + \sigma_y)/2$ [MPa] ($\sigma_z = 0$; plane stress) for following models: a) elongated matrix grains, b) isometric matrix grains, c) isotropic phases, d) circular reinforcement particles.

Hexagonal crystals show differences in thermo-mechanical properties in regard to the crystallographic axes *a* and *c*. Model calculations applied coefficients of thermal expansion (CTE) determined for a single crystal, defining elongation compatible with these axes ($\alpha_{a\text{-}axis}$, $\alpha_{c\text{-}axis}$). Additionally, due to nonlinear CTE changes with the temperature increase, the data coming from a wide range of temperatures were used [25-27]. The modelling with the assumption of isotropic properties of the constituent phases used the mean values of parameters: $(2\cdot\alpha_{a\text{-}axis} + \alpha_{c\text{-}axis})/3$.

All the used material parameters applied for modelling are collected in Table 1.

The application of the real images of composite microstructure imposed two-dimensional geometry of the models. Calculations were performed assuming plane stress. Such an assumption allowed us to verify the results of simulations by comparison with the experimental stress values determined by XRD, neutron diffraction or Raman spectroscopy. The mentioned techniques can help to determine the mean values of thermal residual stress, occurring in the sample surface or in the near-surface layer. For the surface area it can be assumed that the stress perpendicular to that surface is relaxed ($\sigma_\perp \rightarrow 0$) [15] what is close to the simplification of plane stress ($\sigma_\perp = 0$).

Considering anisotropy for a 2-D model (plane stress) demands the use of different calculation techniques, most often applying the local coordinate system (LCS), connected with each grain independently [28-30]. Such a solution was used in the presented models. Additionally, it was assumed that the crystallographic axis *a* for hexagonal symmetry is parallel to the *x* direction in the model and the axis *c* is parallel to the *y* direction. The *z* direction is perpendicular to the plane of microstructure (Fig. 2d).

Directional grain growth in SiC [31] was applied for the LCS orientation of the matrix grains. SiC grains grow in the *a* crystallographic direction, creating plate-like or spherical shapes [32, 33]. The *x* axis in the model was established to be parallel to a longer edge of elongated grains (Fig. 2d). For isometric grains of both SiC and TiB_2 phases the crystallographic orientation was random, but the LCS directions were mostly parallel to the grain edges.

The simulations were conducted assuming thermal loads caused by cooling from 1200°C to 25°C. The simulations assumed also that the stresses existing in the SiC-TiB_2 composite above 1200°C have been relaxed. Such assumptions were also used in the works of other authors [4, 8, 12, 13].

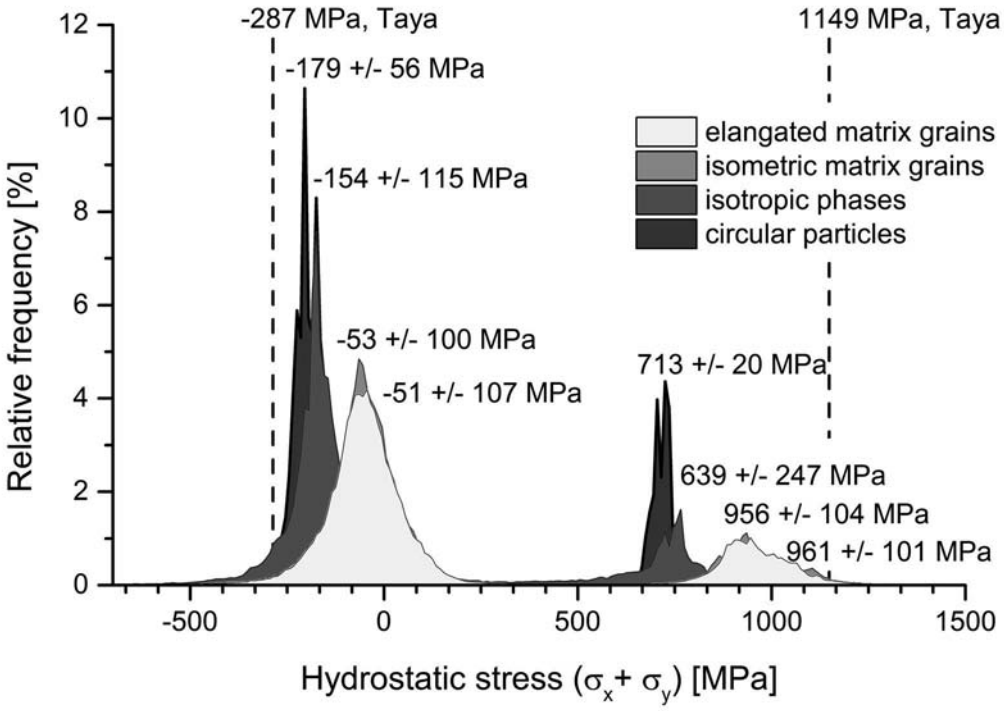

Fig. 4. Histogram of thermal residual stress distribution.

3. Results and discussion

The results of performed simulations of the thermal residual stress distribution were collected in Fig. 3. Stress values were expressed as average hydrostatic stresses ($\sigma_h = (\sigma_x + \sigma_y)/2$; $\sigma_z = 0$; plane stress).

3.1. Elongated and isometric matrix grains

The models, utilizing the real microstructure of SiC-TiB_2 composite with elongated matrix grains, took into account calculations of their anisotropy. The average hydrostatic stresses were calculated for both microstructure variants, comprising elongated and isometric matrix grains (Fig. 3a-3b). The grains of TiB_2 were under tensile stress ($\sigma_h > 0$) due to the larger values of thermal expansion coefficients of the boride phase when compared to the carbide one ($\alpha_p > \alpha_m$). The mean stress values in the TiB_2 grains were of ~ 960 MPa independently on the matrix microstructure.

Fig. 4 shows histograms of the distribution of average hydrostatic stress. The stress distribution in TiB_2 has a large differentiation according to the calculated σ_h values. Standard deviation values exceeded 100 MPa for these grains. It could be caused by the much larger anisotropy of CTE and the much larger values of elastic constants for SiC than for TiB_2 (Table 1). It suggests that the shape of matrix grains and their orientation relative to TiB_2 grains has little influence on the stress distribution in boride inclusions, and the big differentiation of σ_h values in TiB_2 was caused by the CTE anisotropy.

The silicon carbide matrix also showed a wide distribution of mean values. Compressive stresses were dominant due to the relations of CTE's which were described before. Average hydrostatic stresses were on the level of – 50 MPa for both models, differing in grain shapes. For the isometric SiC grains the larger differentiation of stress values occurred. Most probably it is caused by a quantitative factor connected to the larger number of grains with different orientation in the volume unit of the matrix. Average hydrostatic stresses calculated for the presented models were in good agreement with thw experimental data, coming from the thermal residual stress measurements for SiC-TiB_2 composites SiC-TiB_2 [15, 16]. In the composite containing 15.2 vol. % of TiB_2 Winholtz [15] measured by the XRD method microstresses on the level of – 65 MPa and 363 MPa for SiC and TiB_2, respectively. The author of the mentioned work indicated that values of measured stresses strongly depended on the method of sample preparation, and were relaxed by microcracks.

3.2. Anisotropic and isotropic models

In the next elaborated model, assuming isotropic properties of the constituent phases, the real microstructure of SiC-TiB_2 sintered materials was used. Modified material properties were applied to the geometrical model with the isometric matrix. Because of the assumed isotropy the shape of matrix grains had no influence on the results of calculations. The distribution and shape of inclusions remained unchanged which allowed us to compare directly of both the anisotropic and the isotropic model.

The calculated average hydrostatic stresses (Fig. 3c and Fig. 4) were lower for the models with the assumed anisotropy of materials properties. Stress values in TiB_2 grains reached 639 MPa with a large deviation (247 MPa). Such a large differentiation was caused mainly by the difference in TiB_2 grains size. Average stresses in small grains were larger than those calculated for bigger grains. In bigger grains

the stress concentration was observed only near the phase boundary areas.

Average hydrostatic stresses in the carbide matrix were – 154 MPa with a deviation similar to that observed for the anisotropic models. The translation of the maximum of stress distribution to more negative values caused the limitation of areas with the domination of tensile stress ($\sigma_h < 0$). Such results indicate that a simplification of the model, which consists in the application of isotropic parameters of the material for the analysis of its fracture toughness or strength, could lead to a wrong assessment of microcrack and crack deflection effects.

3.3. Real and simplified microstructure

The last investigated model was used to determine the influence of simplification of grains geometry often used in analytical models [8, 17]. Isotropic values of materials properties, the same as for the previously described model, were applied.

The results have indicated the distinct narrowing of the average hydrostatic stress distribution. For TiB_2 grains the standard deviation of σ_h value was more than ten times smaller and for SiC it was twice smaller, when compared to the value calculated in the model basing on the real microstructure. The maximum stress values for both models (Fig. 4) were similar, but the maximal and minimal stress values were much less differentiated. Maximal values of compressive stress in the matrix were – 399 MPa for circle inclusions and for the real microstructure model reached even – 2000 MPa. The similar relation was observed for TiB_2 inclusions. Tensile stress was 754 MPa and 1900 MPa, respectively. Such results indicate that the suggested simplification of the model significantly limited its usage. They also confirm that the grain shape is an important factor influencing the thermal residual stress values in composites.

3.4. Taya and FEA model

Materials parameters collected in Table 1 were used for the calculation of average residual stress, according to equations proposed by Taya [8]. The assumed thermal load was the same as for the previous calculations (1200-20°C). As a result, the average residual stress in TiB_2 was 87 MPa and in SiC 1149 MPa. A comparison of the calculated values with values coming from the modelling led to the statement that they are limit values (Fig. 4).

4. Conclusions

The models presented in this work, based on the real SiC-TiB_2 composite microstructure, allowed the authors to determine the influence of grains shape and thermo-mechanical properties anisotropy on thermal residual stresses in this material.

The results of the performed simulations were in good agreement with the empirical data. A comparison of thermal residual stress values, achieved for the models applying anisotropy or isotropy of material properties and basing on real or simplified geometry of the microstructure, clearly indicates that these models are non-comparable. The results achieved with different models were distinctly different.

Acknowledgements

This work was financially supported by Polish State Ministry of Science and Higher Education under AGH University project no. 11.11.160.617.

The research was supported in part by PLGrid Infrastructure.

References

[1] Munro, R. G.: Material Properties of a Sintered α-SiC, *J. Phys. Chem. Ref. Data*, 26, (1997), 1195-1203, doi:10.1063/1.556000.

[2] Gubernat, A., Stobierski, L., Łabaj, P.: Microstructure and mechanical properties of silicon carbide pressureless sintered with oxide additives, *J. Eur. Ceram. Soc.*, 27, (2007), 781-789, doi:10.1016/j.jeurceramsoc.2006.04.009.

[3] Snead, L. L., Nozawa, T., Katoh, Y., Byun, T. S., Kondo, S., Petti, D. A.: Handbook of SiC properties for fuel performance modeling, *J. Nucl. Mater.*, 371, (2007), 329-377, doi:10.1016/j.jnucmat.2007.05.016.

[4] King, D. S., Fahrenholtz, W. G., Hilmas, G. E.: Silicon carbide-titanium diboride ceramic composites, *J. Eur. Ceram. Soc.*, 33, (2013), 2943-2951, doi:10.1016/j.jeurceramsoc.2013.03.031.

[5] Grabowski, G., Stobierski, L., Rutkowski, P.: Internal sources of damage in ceramic materials, *Ceramika/Ceramics*, 97, (2006), 293-298.

[6] Górny, G., Stobierski, L., Rutkowski, P., Rączka, M.: Effect of Processing Conditions on Microstructure of SiC-TiB_2 Composite, *Solid State Phenom.*, 197, (2013), 250-255, doi:10.4028/www.scientific.net/SSP.197.250.

[7] Khaund, A. K., Krstic, V. D., Nicholson, P. S.: Influence of elastic and thermal mismatch on the local crack-driving force in brittle composites, *J. Mater. Sci.*, 12, (1977), 2269-2273, doi:10.1007/BF00552248.

[8] Taya, M., Hayashi, S., Kobayashi, A. S. A. S., Yoon, H. S. S.: Toughening of a Particulate-Reinforced/Ceramic-Matrix Composite, *J. Am. Ceram. Soc.*, 73, (1989), 1382-1391, doi:10.1111/j.1151-2916.1990.tb05209.x.

[9] Yoon, J. D., Kang, S. G.: Strengthening and toughening behaviour of SiC with additions of TiB_2, *J. Mater. Sci. Lett.*, 14, (1995), 1065-1067, doi:10.1007/BF00258166.

[10] K.-S. Cho, Y.-W. Kim, H.-J. Choi, J.-G. Lee: SiC-TiC and SiC-TiB_2 composites densified by liquid-phase sintering, *J. Mater. Sci.*, 31, (1996), 6223-6228, doi:10.1007/BF00354442.

[11] Kim, Y., Mitomo, M., Hirotsuru, H.: Microstructural Development of Silicon Carbide Containing Large Seed Grains, *J. Am. Ceram. Soc.*, 80, (1997), 99-105, doi:10.1111/j.1151-2916.1997.tb02796.x.

[12] Blanc, C.,Thevenot, F., Goeuriot, D.: Microstructural and mechanical characterization of SiC-submicron TiB_2 composites, *J. Eur. Ceram. Soc.*, 19, (1999), 561-569, doi:10.1016/S0955-2219(98)00227-1.

[13] Bucevac, D., Matovic, B., Boskovic, S., Zec, S., Krstic, V.: Pressureless sintering of internally synthesized SiC-TiB_2 composites with improved fracture strength, *J. Alloys Compd.*, 509, (2011), 990-996, doi:10.1016/j.jallcom.2010.09.152.

[14] Wei, G. C., Becher, P. F.: Improvements in Mechanical Properties in SiC by the Addition of TiC Particles, *J. Am. Ceram. Soc.*, 67, (1984), 571-574, doi:10.1111/j.1151-2916.1984.tb19174.x.

[15] Winholtz, R. A., Separation of Microstresses and Macrostresses, in: M. T. Hutchings, A. D. Krawitz (Eds.), *Meas. Residual Appl. Stress Using Neutron Diffr.*, Springer Netherlands, Dordrecht, 1992, 131-145. doi:10.1007/978-94-011-2797-4_8.

[16] Oden, M.: *Residual Stress in Ceramics and Ceramic Composites*, Linköping University, 1992.

[17] Selsing, J.: Internal Stresses in Ceramics, *J. Am. Ceram. Soc.*, 44, (1961), 419-419, doi:10.1111/j.1151-2916.1961.tb15475.x.
[18] Stobierski, L., Gubernat, A., Sintering of silicon carbide I. Effect of carbon, *Ceram. Int.*, 29, (2003), 287-292, doi:10.1016/S0272-8842(02)00117-7.
[19] L. Stobierski, A. Gubernat, Sintering of silicon carbide II. Effect of boron, *Ceram. Int.* 29 (2003) 355-361, doi:10.1016/S0272-8842(02)00144-X.
[20] Li, Z., Bradt, R.C.: The single crystal elastic constants of hexagonal SiC to 1000°C, *Int. J. High Technol. Ceram.*, 4, (1988), 1-10, doi:10.1016/0267-3762(88)90060-4.
[21] Spoor, P., Maynard, J., Pan, M., Green, D., Hellmann, J., Tanaka, T.: Elastic constants and crytal anisotropy of TiB_2, *Appl. Phys. Lett.*, 70, (1997), 1959-1961, doi:10.1063/1.118791.
[22] Sakaguchi, S., Murayama, N., Kodama, Y., Wakai, F.: The Poisson's ratio of engineering ceramics at elevated temperature, *J. Mater. Sci. Lett.*, 10, (1991), 282-284, doi:10.1007/BF00735658.
[23] Munro, R. G.: Material properties of titanium diboride, *J. Res. Natl. Inst. Stand. Technol.*, 105, (2000), 709-720, doi:10.6028/jres.105.057.
[24] Hill, R.: The elastic behaviour of a crystalline aggregate, *Proc. Phys. Soc. Sect. A*, 349, (1952), 349.
[25] Li, Z., Bradt, R. C., Thermal expansion of the hexagonal (6H) polytype of silicon carbide, *J. Am. Ceram. Soc.*, 66, (1986), 863-866, doi:10.1111/j.1151-2916. 1986.tb07385.x.
[26] Inoue, Z.: Kurachi, Y.: Structure Change of SiC at High Temperature, in: S. Somiya, E. Kanai, K. Ando (Eds.), in *Proc. Int. Symp. Ceram. Components Engines*, KTK Scientific Publisher, Tokyo, 1983, 519-527.
[27] Touloukian, Y. S., Kirby, R. K., Taylor, R. E., Lee, T. Y. R.: Thermophysical Properties of Matter: Thermal Expansion of Nonmetallic Solids, *IFI/Plenum*, 1977.
[28] Espinosa, H. D., Zavattieri, P. D.: A grain level model for the study of failure initiation and evolution in polycrystalline brittle materials. Part I: Theory and numerical implementation, *Mech. Mater.*, 35, (2003), 333-364, doi:10.1016/S0167-6636(02)00285-5.
[29] Sfantos, G. K., Aliabadi, M. H.: Multi-scale boundary element modelling of material degradation and fracture, *Comput. Methods Appl. Mech. Eng.*, 196, (2007), 1310-1329, doi:10.1016/j.cma.2006.09.004.
[30] Kim, K., Geringer, J., Macdonald, D. D.: Crack simulation of nano-bioceramic composite microstructures with cohesive failure law: effects of sintering, loads and time, *J. Mech. Behav. Biomed. Mater.*, 15, (2012), 1-12, doi:10.1016/j.jmbbm.2012.07.003.
[31] Tanaka, H., Hirosaki, N., Nishimura, T., D.-W. Shin, S.-S. Park: Nonequiaxial Grain Growth and Polytype Transformation of Sintered α-Silicon Carbide and β-Silicon Carbide, *J. Am. Ceram. Soc.*, 86, (2003), 2222-2224, doi:10.1111/j.1151-2916.2003.tb03638.x.
[32] G.-D. Zhan, Mitomo, M., Y.-W. Kim: Microstructural Control for Strengthening of Silicon Carbide Ceramics, *J. Am. Ceram. Soc.*, 82, (2004), 2924-2926, doi:10.1111/j.1151-2916.1999.tb02181.x.
[33] Wereszczak, A. A., Lin, H. T., Gilde, G. A.: The effect of grain growth on hardness in hot-pressed silicon carbides, *J. Mater. Sci.*, 41, (2006), 4996-5000, doi:10.1007/s10853-006-0110-z.

♦

Received 16 October 2015, accepted 27 January 2016.